

LCLS INJECTOR LASER MODULATION TO IMPROVE FEL OPERATION EFFICIENCY AND PERFORMANCE

S. Li*, D. Bohler, J. Corbett, A.S. Fisher, S. Gilevich, Z. Huang, A. Li, D. Ratner,
J. Robinson, F. Zhou, SLAC, Menlo Park, CA 94025, USA
R. Fiorito, E. Montgomery, University of Maryland, College Park, MD 20742, USA
H. Zhang, Cockcroft Institute and University of Liverpool, Warrington, WA44AD, UK

Abstract

In the Linear Coherent Light Source (LCLS) at SLAC, the injector laser plays an important role as the source of the electron beam for the Free Electron Laser (FEL). The injector laser strikes a copper photocathode which emits photo-electrons due to photo-electric effect [1]. The emittance of the electron beam is highly related to the transverse shape of the injector laser. Currently the LCLS injector laser has hot spots that degrade the FEL performance. The goal of this project is to use adaptive optics to modulate the transverse shape of the injector laser, in order to produce a desired shape of electron beam. With a more controllable electron transverse profile, we can achieve lower emittance for the FEL, improve the FEL performance and operation reliability. We first present various options for adaptive optics and damage test results. Then we will discuss the shaping process with an iterative algorithm to achieve the desired shape, characterized by Zernike polynomial deconstruction.

INTRODUCTION

The injector laser of a Free Electron Laser (FEL) is a source to produce electron beams which are then accelerated to relativistic speed and generate coherent radiation in the undulator. At Linear Coherent Light Source (LCLS) at SLAC, the injector laser consists of a Ti:Sapphire laser system, producing 2 ps laser pulses at 760 nm wavelength. The infrared laser is then converted to ultraviolet wavelength (253 nm) via nonlinear process in a frequency tripler. The laser strikes a copper photocathode which emits photo-electrons due to the photo-electric effect [1].

Currently the LCLS injector laser has hot spots in its transverse profile. Figure 1 is a typical example of the transverse profile of the LCLS injector laser (left) and electron beam (right) near cathode. Non-uniformities in laser profile and cathode quantum efficiency lead to the non-uniformities in electron beam, which increase the electron beam emittance in the downstream linac and FEL. Lower emittance electron beam can enhance FEL performance. Other studies have shown certain types of laser transverse profile lead to lower electron emittance [2, 3]. Therefore, with adaptive optics, we can distinguish two major advantages. One is to remove non-uniformities in the electron beam, and the other is to shape the beam into an arbitrary profile [4].

In this paper, we present various options for the adaptive optics to modulate the injector laser, and show damage

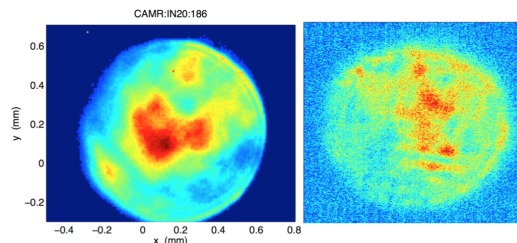


Figure 1: Example of LCLS injector laser transverse profile (left). Example of electron beam transverse profile (right).

test results for these materials. We also discuss the shaping process with an iterative algorithm, in which Zernike polynomial reconstruction is used to characterize the transverse shape of the laser.

ADAPTIVE OPTICS

There are various options for adaptive optics. We have considered Digital Micro-mirror Device (DMD), liquid crystal Spatial Light Modulator (SLM), and Deformable Mirror (DM). These materials have different properties and work in different wavelength ranges. In this section we will briefly describe how each device works and present damage test results.

Infrared (IR) Beam: DMD and SLM

The diagram of the damage test is shown in Fig. 2. The test was done at the HOLE laser lab at SLAC, with a laser identical to the LCLS injector laser. The laser is a 2 ps pulsed laser at 760 nm wavelength 120 Hz. The waveplate and polarizer allow us to tune the laser beam energy. The iris cuts the beam and is imaged through a lens onto the sample plane. The beam energy varies from 20 μ J to 1 mJ. At the image plane we replaced the camera with the sample and let the laser hit the chip at different spots for an exposure time up to 40 minutes. We gradually increased the beam energy and moved the sample across the surface until we saw visible damage on the pixels. Then we took the sample to the microscope lab and looked at the damage under microscope.

The Texas Instrument DLP7000 is a DMD made of an array of micro-mirrors. When powered on, each individual micro-mirror can deflect at $\pm 12^\circ$ angle. The shaping process is done by grouping individual micro-mirrors to macro-mirrors which consist of, for example, 5×5 micro-mirrors. For a certain macro-mirror, we can randomly turn off a number of micro-mirrors according to the ratio of cur-

* siqili@slac.stanford.edu

Content from this work may be used under the terms of the CC BY 3.0 licence (© 2015). Any distribution of this work must maintain attribution to the author(s), title of the work, publisher, and DOI.

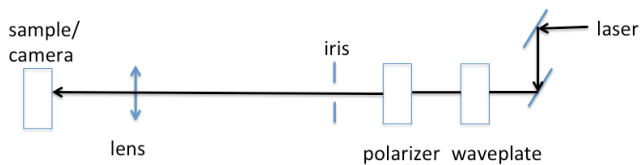


Figure 2: Damage test diagram for DMD and SLM at the sample location.

rent intensity to desired intensity. Thus a portion of the original laser is deflected away from the beam path. The overall effect can smooth out the transverse profile of the laser and shape the beam into an arbitrary profile.

We calibrated the camera image with the total beam energy to get fluence per pixel. With the DMD powered off, we take the damage threshold to be the peak fluence for a beam energy where we just start to see damage. Figure 3 shows the microscope images of the damaged pixels. For this test the threshold fluence is 20.7 mJ/cm^2 . The uncertainty in this measurement comes from how well we can measure the beam size, which depends on how well we align the sample with the image plane where we take the camera image. With an uncertainty of $\pm 1 \text{ mm}$, we moved the camera relative to the image plane and measured the change in fluence, giving the damage threshold fluence $20.7 \pm 2.4 \text{ mJ/cm}^2$.

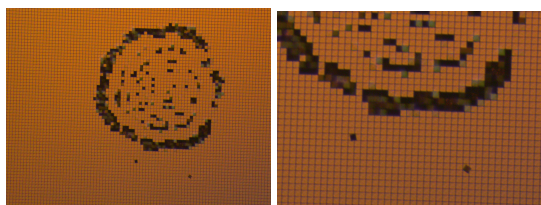


Figure 3: Microscope images of damaged DMD pixels, zoomed in on the right.

SLM are commercially available liquid crystal panels that can do phase and amplitude modulations on laser beam. We received a sample from Holoeye Photonics AG for the IR wavelength range. We followed the same test diagram and method described in the previous subsection to study the damage threshold (Fig. 4). The damage fluence threshold is found to be $28.0 \pm 2.9 \text{ mJ/cm}^2$.

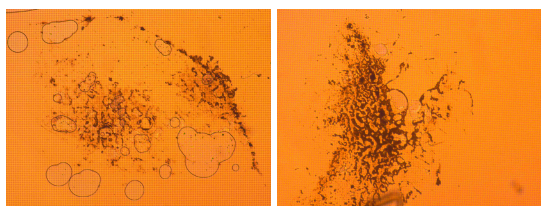


Figure 4: Damaged liquid crystal SLM panel for laser pulse energy $700 \mu\text{J}$ (left) and 1 mJ (right).

Ultraviolet (UV) Beam: DM

We also did damage tests on DM samples made of aluminum and dielectric material. These materials can work in

the UV wavelength range, so we built a tripler for the test, as shown in Fig. 5. With the tripler, the maximum beam energy is $150 \mu\text{J}$, and we did not see any visible damage under microscope. The peak fluence is 31.4 mJ/cm^2 , so the damage threshold is above this value.

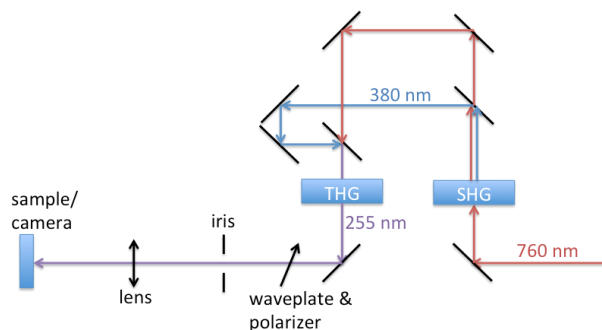


Figure 5: Tripler set up for the DM damage test.

SHAPING ALGORITHM

The shaping process is done in an iterative manner, illustrated in Fig. 6. We start out with an input laser image taken by the camera. Then we produce a mask to put on adaptive optics to modulate the transverse shape of the beam. This produces an output image that we can analyze. There are many different ways to characterize what is a "good" shape. In following paragraphs we will discuss the method of Zernike polynomial reconstruction. If this image satisfies the condition to be a good shape, then the process is finished. Otherwise, this output image will be used as an input image to produce another mask. Then this process repeats itself until the criterion is satisfied.

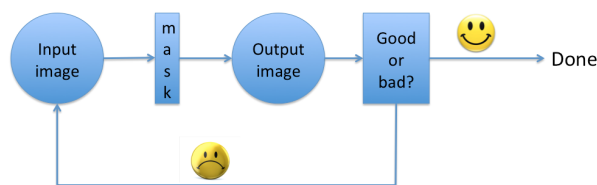


Figure 6: Diagram to illustrate the iterative process of laser shaping.

We have conducted preliminary tests using a DMD chip and a diode IR laser. In this example, we try to get a flat-top transverse laser profile. Figure 7 left is the original transverse profile of the diode laser. Figure 7 middle is the profile after first iteration, and Fig. 7 right is the profile after second iteration. One can see that part of the hot spots are being smoothed out by DMD pixels.

Aside from flat-top, the DMD is also capable of shaping the beam into Gaussian, parabolic, and any arbitrary shape defined by the user. In Fig. 8, we shape the beam to a parabolic profile. The line-out across the centroid of the beam (second row of Fig. 8) shows the change in the overall shape.

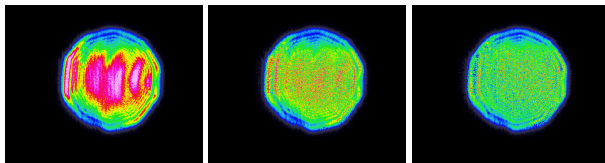


Figure 7: Left: original profile. Middle: profile after first iteration. Right: profile after second iteration.

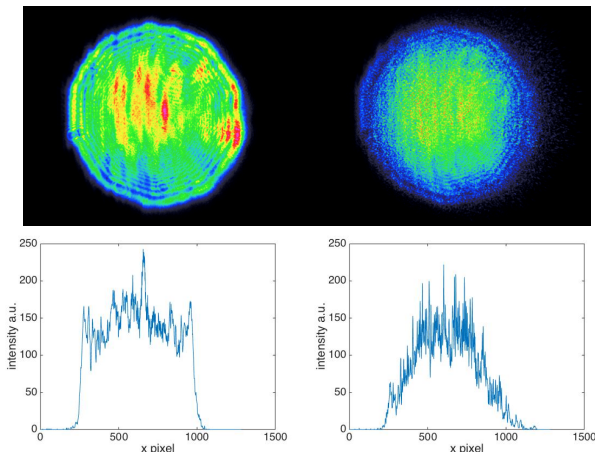


Figure 8: Upper row from left to right: original beam profile to parabolic profile after one iteration. Lower row: line-out across the centroid of the beam.

Zernike Polynomial Reconstruction

As mentioned above, we need a criterion to characterize the transverse profile of the beam for the iteration process. One way of doing it is to use Zernike polynomials. Zernike polynomials are functions that form an orthogonal basis on the unit circle. Zernike reconstruction breaks down the original image into components of Zernike polynomials, giving each polynomial an associated coefficient to describe its contribution [5]. The more polynomials we use, the more accurate the reconstruction is relative to the original profile. Figure 9 shows the original profile and three reconstructions using different numbers of polynomials. With proper normalization, the coefficients should add up to unity. Ideally, the beam is composed only of circularly symmetric polynomials. In this test we use the first 210 polynomials to reconstruct the profile, and calculate the sum of first five circularly symmetric polynomials, namely the 1st, 5th, 13th, 25th, and 41st, to compare to 1. In Fig. 7, the sum of these coefficients from left to right are 0.8276, 0.8863, 0.9148, increasing as the profile improves. In the iterative algorithm, for example, we can use 0.9 as the threshold to stop the iteration. There are also other mathematical expressions to characterize the transverse beam profile using Zernike polynomials. For example, if one would like to create a parabolic beam shape, then the 5th polynomial is of essential importance.

The iterative algorithm is currently a work in progress. We will do more tests when we commission the DMD in the injector laser.

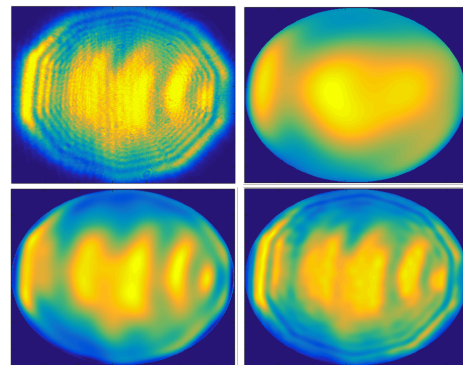


Figure 9: Upper left: original profile. Upper right: reconstruction using 45 polynomials. Lower left: reconstruction using 210 polynomials. Lower right: reconstruction using 1035 polynomials.

CONCLUSION

In this paper we have presented the principle and preliminary results of LCLS injector laser modulation. Three options of adaptive optics are under investigation, in terms of damage threshold and feasibility to work in the LCLS injector lab. We found the damage threshold fluence to be $20.7 \pm 2.4 \text{ mJ/cm}^2$ for the DMD, and $28.0 \pm 2.9 \text{ mJ/cm}^2$ for the SLM, at 760 nm wavelength. For the DM at 253 nm wavelength, we did not see damage with maximum fluence 31.4 mJ/cm^2 . We have described the iterative algorithm for the shaping, with a goal to correct for non-uniformities in the injector laser and cathode quantum efficiency map, and to shape the beam into any arbitrary profile. Zernike polynomials are used to characterize the beam profile. Currently, we are exploring DMD in the UV wavelength range, and designing optical configuration to accommodate for the change in the set up.

REFERENCES

- [1] Akre, R., et al. "Commissioning the linac coherent light source injector", *Physical Review Special Topics-Accelerators and Beams* 11.3 (2008): 030703.
- [2] Zhou, Feng, et al. "Impact of the spatial laser distribution on photocathode gun operation." *Physical Review Special Topics-Accelerators and Beams* 15.9 (2012): 090701.
- [3] Brachmann, A., et al. "LCLS drive laser shaping experiments." *Proceedings of the International Free-Electron Laser Conference 2009, Liverpool, UK*, pp. 463 - 465.
- [4] Maxson, Jared, et al. "Adaptive electron beam shaping using a photoemission gun and spatial light modulator." *Physical Review Special Topics-Accelerators and Beams* 18.2 (2015): 023401.
- [5] Padilla-Vivanco, Alfonso, Areli Martinez-Ramirez, and Fermin-Solomon Granados-Agustin, "Digital image reconstruction using Zernike moments", *Remote Sensing International Society for Optics and Photonics*, (2004)